

Observation of Confined Current Structures in JET High Temperature Pedestals and Transient ELM Suppression

E.R Solano 1), P.J. Lomas 2), B. Alper 2), G. Arnoux 2), A. Boboc 2), L. Barrera 1), P. Belo 3), M.N.A. Beurskens 2), M. Brix 2), K. Crombe 4), E de la Luna 1), S. Devaux 5), T. Eich 5), S. Gerasimov 2), C. Giroud 2), D. Harting 6), D. Howell 2), G. Kocsis 7), H. R. Koslowski 6), Y. Liang 6), A. López-Fraguas 1), M.F.F. Nave 3), E. Nardon 11), C. Pérez von Thun 6,9), S.D. Pinches 2), E. Rachlew 8), F. Rimini 9), S. Saarelma 2), A. Sirinelli 2), H. Thomsen 5), G.S. Xu 11), L. Zabeo 12), D. Zarzoso 10) and JET EFDA contributors* .

E-mail contact of main author: emilia.solano@ciemat.es

JET-EFDA, Culham Science Centre, Abingdon, OX14 3DB, UK

1) Asociación EURATOM-CIEMAT, 28040, Madrid, Spain; 2) Euratom/CCFE Fusion Association, Culham Science Centre, Abingdon, OX14 3DB, UK; 3) Associação EURATOM/IST, IPFN, Av Rovisco Pais, 1049-001, Lisbon, Portugal; 4) Department of Applied Physics, Ghent University, Rozier 44, 9000 Gent, Belgium; 5) Max-Planck-Institut für Plasmaphysik, EURATOM-Assoziation, Garching and /Greifswald, Germany; 6) Forschungszentrum Jülich GmbH, Institut für Plasmaphysik, EURATOM-Assoziation, TEC, D-52425 Jülich, Germany; 7) KFKI RMKI, Association EURATOM, P.O.Box 49, H-1525, Budapest, Hungary; 8) Association EURATOM-VR, Department of Physics, SCI, KTH, SE-10691 Stockholm, Sweden; 9) EFDA Close Support Unit, Culham Science Centre, Culham, OX14 3DB, UK; 10) Association EURATOM-CEA, CEA/DSM/IRFM, Cadarache, 13108 Saint Paul Lez Durance, France; 11) Inst. of Plasma Physics, Chinese Academy of Sciences, Hefei 230031, China; 12) ITER Organisation, Cadarache, 13108 Saint Paul Lez Durance, France

Abstract. We report the identification of a localized current structure inside the JET plasma. It is a field aligned closed helical ribbon, carrying current in the same direction as the background current profile (co-current), rotating toroidally with the ion velocity (co-rotating). It appears to be located at an $n=1$ rational surface at a flat spot in the plasma pressure profile, at the top of the pedestal, and not in the gradient region. The current structure appears spontaneously in low density, high pedestal temperature, high rotation plasmas, and can last up to 1. s, a time comparable to a local resistive time. It considerably delays the appearance of the first ELM, and regulates transport across the separatrix.

1. Introduction

Recent experiments at JET were designed to explore plasmas with high temperature pedestals, similar to the values presently expected for ITER. In JET this is most easily achieved in a transient manner by reducing particle fuelling (from external sources and wall) and operating at initially low density in the hot ion H-mode regime [1]. The transition to H-mode occurs at low plasma density. After that the pedestal density, rotation and temperatures rise up until the occurrence of the first natural ELM. In recent cases the electron temperature at the top of the pedestal can reach up to $T_{e,ped} = 2.8$ keV before the first ELM, although higher values have been reported in the past. In these plasma conditions the pedestal stability can be qualitatively different to the usual ELMy H-mode situation, as evidenced by the appearance of multi-harmonic Outer Modes (MH-OMs). Outer Mode is

* See the Appendix of F. Romanelli et al., paper OV/1-3, this conference

the name given in JET to kink-like instabilities outside of the $q=2$ surface [2,3,4]. Sometimes the name OM is used to describe multi-harmonic features and sometimes not, which is why in this paper we will use the MH modifier to single out the type of mode we are referring to.

We identify the observed MH-OMs as radially confined current filaments or ribbons, co-rotating with the plasma [5]. These current structures lead to a quasi-stationary state in which ELMs are suppressed or delayed.

2. Experimental observations and characterization

A very characteristic signature of the MH-OMs is the harmonic structure of the fast Fourier transform (FFT) of the Mirnov signals, shown in Fig 1g (other plots in that figure will be described later). In the pulse of Fig. 1 the fundamental frequency is $f \sim 6$ kHz

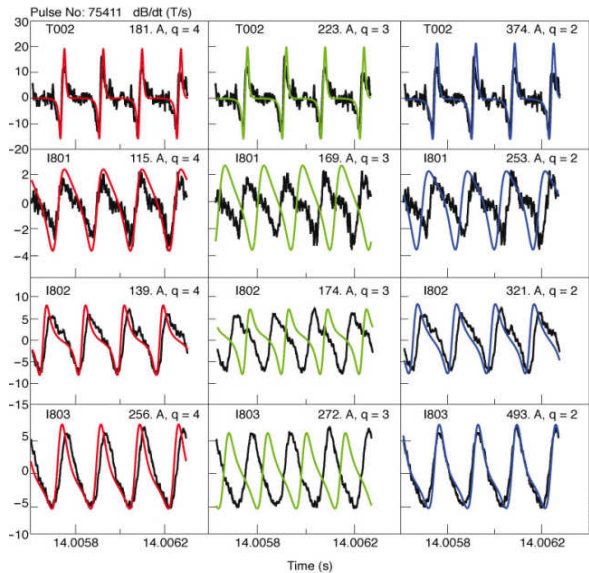


Fig. 2: Comparison of data (black) from Mirnov coils with simulated signals generated with rotating current ribbons located at $q=4$ (red), $q=3$ (green) and $q=2$ (blue) flux surfaces. Coils are located at the plasma outboard (top row), and three inboard coils (above, near and below the plasma midplane, respectively). Reprinted figure with permission from E.R. Solano et al., Phys. Rev. Lett. 104, 185002 (2010)

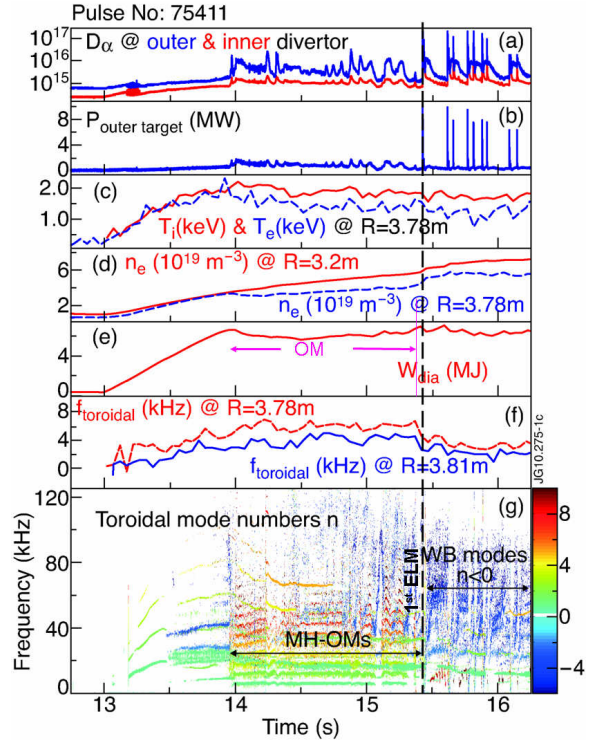


Fig. 1: time traces showing a long-lived Outer Mode, starting from 14 s to 15.38s, and its effect on plasma behaviour: a) rise in D_α ; b) rise in power to outer target; c) drop in pedestal temperatures; d) slower pedestal density rise, rising core density; e) stationary energy; f) toroidal rotation frequency at top and middle of pedestal g) contour plot of toroidal mode numbers of Mirnov signal spectrum.

and every subsequent harmonic has n increased by 1. Harmonics are seen up to 45 kHz ($n=7$), but the mode is at times clearly recognisable up to 90 kHz ($n=15$). Multiple harmonics are observed in all Mirnov probes around the plasma, and in many fluctuation diagnostics in the pedestal region.

Discrete blips observed in the Mirnov signals indicate the presence of a localised current structure, rotating in the same direction as the ions in the plasma and carrying excess current relative to the axisymmetric equilibrium current profile. Since the current feature is long-lived (>1 s), it must be located inside the magnetic separatrix. Since $n=1$ and the fundamental frequency is narrow, it must be composed of closed field lines, aligned

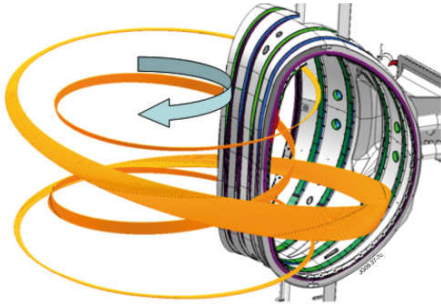


Fig.3: $q=4$ current ribbon that provides best fit to magnetic signals from Mirnov coil set, with current 100-200 A. Reprinted figure with permission from E.R. Solano et al., *Phys Rev Lett* 104 185003 (2010)

with the magnetic field at a rational surface. Plotted in Fig. 2 is a comparison of measured magnetic signals at various poloidal locations with simulated signals produced by assuming a field-aligned current ribbon located at the $q=4$, 3 and 2 surfaces. The current values quoted in each plot are the current carried by the ribbon, adjusted to match signal amplitude. The scatter in simulated current values is representative of uncertainties in reconstruction of the plasma shape. Comparison of the shapes and phases of measured and simulated signals shows that the current structure is best simulated as a current ribbon with excess current of 100-300 A (plasma current is 2.5 MA), with toroidal mode number $n=1$, poloidal mode number $m=4$, and toroidal width of the order 5-10% of the toroidal circumference of the plasma, rotating toroidally at 6 kHz. Odd values of q cannot fit the inboard data. Outboard coils, although more numerous provide insufficient information to select m . The width of the ribbon is determined by the fastest observed change in dB/dt , and it is clearly resolved. Data in one inboard coil is substantially better fitted with $q=4$, rather than by $q=2$. Further, the $q=2$ flux surface is too far inboard to match the rotation frequency of the mode, and the fluctuation measurements detect no sign of the MH-OM so far inboard. Therefore we conclude the OM is a field-aligned structure at $q=4$. A representation of the $q=4$ current ribbon that best matches the data is shown in Fig. 3. MH-OMs have also been observed with $q=5$.

Characteristic profiles at the onset ($t=14$ s) of the OM phase are shown in Fig. 4. We identify the radial position of the current ribbon as the location where toroidal rotation frequency matches mode frequency. From the start of the OM it appears that the location of the mode is at the edge of the ion rotation gradient region, at the flat-top of the density

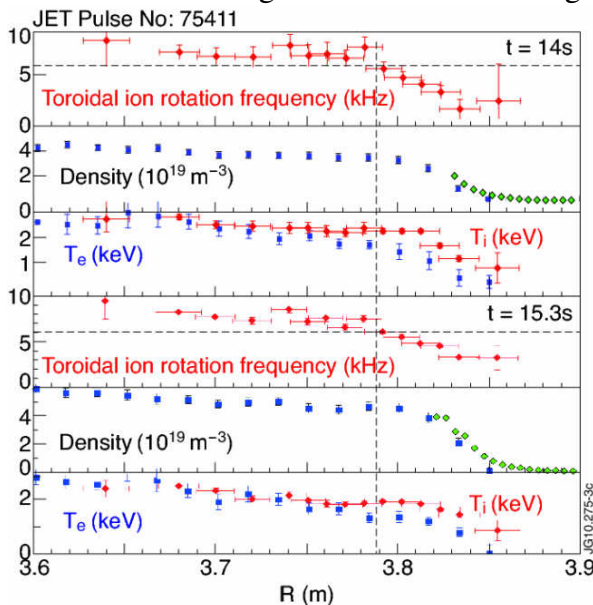


Fig. 4: profiles of toroidal rotation frequency, n_e , T_e , T_i at start (top 3 plots) and end (lower 3 plots) of OM. Vertical line marks position where mode and plasma rotation frequencies are equal.

pedestal, inboard of the maximum pressure gradient, probably at a pressure flat-top. Because the rotational shear is high around 6 kHz, the current structure must be well localised in the radial direction. At the end of this MH-OM (15.3 s) the toroidal rotation shear is somewhat eroded. The edge charge-exchange diagnostic has an averaging time window of 50 ms, so only longer-lived OMs can be checked. The radial localisation of the MH-OM at the flat-top of the pedestal is observed in all cases checked. At the pedestal flat-top force balance is special: locally the equilibrium is force-free and local helicity is a conserved quantity. This may explain why MH-OMs are so long-lived. It also relates MH-OMs to snakes [6], observed at the foot of ITB barriers, and palm-tree

modes [7], observed equally at the pedestal flat-top.

Fluctuations of electron cyclotron emission in the T_e gradient region, X-mode reflectometry and edge channels of Soft X-Rays, as well as the edge interferometer all show at least 3 harmonics of the OM. All these fluctuations measurements are sensitive to the flux surface deformation introduced by the current structure. The data is compatible with earlier studies [3] that established the non-tearing character of the OM: a tearing mode would exhibit alternating flat and steep profiles as the magnetic island moves past the measuring channels. These are not observed.

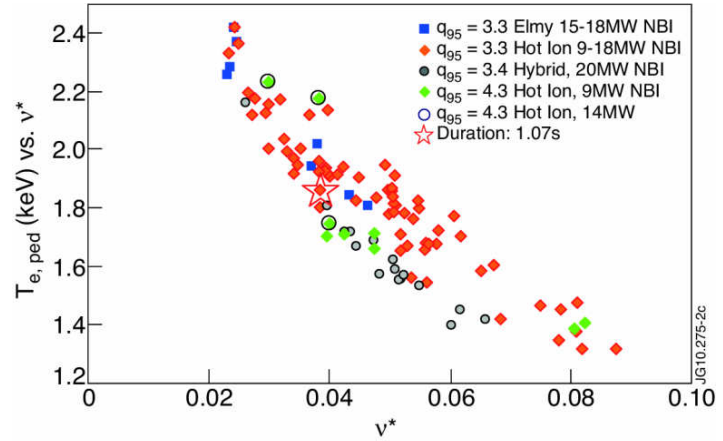


Fig. 5: $T_{e,ped}$ vs. pedestal collisionality ν^* at the onset of the MH-OMs.

a tearing mode would exhibit alternating flat and steep profiles as the magnetic island moves past the measuring channels. These are not observed.

3. Operating space and effects on plasma

The plasmas in which $n=1$ MH-OMs were observed at JET all had high triangularity ($\delta=0.4$), 2-3 MA of plasma current, 2.-3.3 T toroidal field, and 9-20 MW of co-injected Neutral Beam Injection (NBI) heating. Although MH-OMs were initially observed in the Hot Ion H-mode regime, they were also found in standard ELMy H-mode and in hybrid plasmas. Only MH-OMs with $n=1$ fundamental mode number and with at least 2 visible harmonics in soft X-rays are presented. Representative values of $T_{e,ped}$ vs. pedestal top collisionality, ν^* , at the start of the mode are shown in Fig. 5. MH-OMs are only observed when $n_{e,ped}/n_{GW}=0.4\pm 0.1$, with $5\times 10^{19} \text{ m}^{-3} < n_{e,ped} < 5\times 10^{19} \text{ m}^{-3}$, $T_{e,ped} > 1.2 \text{ keV}$, $T_{i,ped} > 1.4 \text{ keV}$, $\nu^* < 0.09$. Note that ITER pedestal temperatures, early in the H-mode phase, are presently expected to be in of order 2-5 keV, with $n_{e,ped} \sim 3.5\text{-}7\times 10^{19} \text{ m}^{-3}$, $n_{e,ped}/n_{GW}=0.3\text{-}0.6$ and $\nu^* \sim 0.02\text{-}0.1$, clearly in the same range. Steady ELMy H-mode plasmas with similar currents and fields typically have $T_{e,ped} < 1.5 \text{ keV}$, $\nu^* > 0.05$. We do not know yet the physics behind the formation of MH-OMs: plasmas with $n_{e,ped}$, $T_{e,ped}$ in the same range often do not have MH-OMs. Therefore plasma shape, pedestal height, resistivity or collisionality do not, by themselves, determine pedestal MHD behavior.

In most cases the fundamental mode frequency of the MH-OM is between 3.7 and 7.3 kHz, and often near 6 kHz. The two modes in a hot ion pulse with $q=5$ at the pedestal top that reached 2.2 keV had high current and field (2.5 MA, 3.3 T) and unusually high frequency: 9.5 kHz. No scaling of mode frequency with plasma bulk parameters was found.

Ramps of plasma current of order 0.2 MA/s in either direction prevent appearance of OM in pulses that were otherwise repeats of pulses with spontaneous modes. This contradicts the view that OMs are kinks driven by edge current density and would therefore be favored by an upwards current ramp. It again confirms that localization of a resonant q at the flat-top of the pedestal is an important ingredient for mode formation.

Of the 103 MH-OMs identified, 64 were terminated by an ELM. It is possible that technical details of plasma evolution contribute to reduce mode life-time: a slow plasma radial drift is

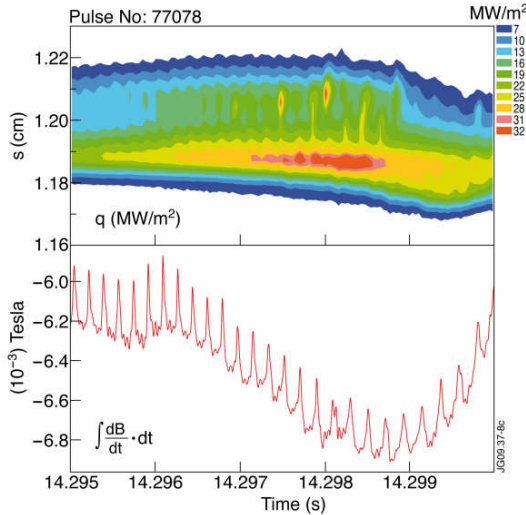


Fig. 6: heat flux contours at outer strike, measured with IR, and integrated magnetic signal showing correlation of heat pulses with rotation of current structure. Reprinted figure with permission from E.R. Solano et al., Phys. Rev. Lett. 104, 185003 (2010)

have also been observed in earlier reversed field experiments (which in JET implies counter NBI). When ion cyclotron resonance heating (ICRH) is applied there are sometimes external kinks with higher frequencies, and $n=2$ or 3 fundamental mode numbers. These modes are much more difficult to study, as they often coincide in frequency with $n=1$ core modes. It is not clear if ICRH suppresses the MH-OMs or simply renders them difficult to detect or identify.

Let us now consider the detailed time evolution of the longest MH-OM in the database, shown in Fig. 1. The profile quantities are taken at $R=3.78$ m, at the top of the pedestal, inboard of the pedestal knee. The mode spectrum was already discussed. After the transition to H-mode, marked by the initial D_α drop at $t=13.2$ s, the pedestal quantities rise as usual in an H-mode, until the MH-OM begins at the time $t=13.98$ s. Then D_α rises substantially, $T_{e,ped}$ begins to drop, and the toroidal rotation frequency at the pedestal becomes nearly constant. Density continues to rise, albeit slower than before, and pressure at the pedestal top remains fairly constant. The H factor drops down from a maximum value of $H_{98}=1.4$ to a steady value of $H_{98}=1.1$ at the outset of the OM. Impurity content during the OM is normal compared to a medium density ELMy H-mode: $Z_{eff} \sim 1.5-2$. The MH-OM survives 2 sawtooth crashes (at 14.23 and 14.87 s), indicating that it is a robust feature of the plasma, although at times it disappears and returns again. After the \hat{r}^t ELM the pedestal rotation frequency drops below 4 kHz and the OM does not return. In this case there is a brief quiet interval between the end of the MH-OM at 15.375s and the ELM at 15.430 s. This first ELM causes an impurity influx, the density rises and the MH-OM does not return. In about 60% of the OMs observed in the 2008-2009 experimental campaigns the OMs are terminated by ELMs. Sometimes MH-OMs return with ever decreasing duration some hundreds of ms after the first few ELMs. The MH-OM often appears when recycling and gas fuelling are particularly low, and it can be reduced or eliminated by increased fuelling. For example, a recent pulse with the same conditions as in Fig. 1 but with more fuelling ($1.9 \cdot 10^{21}$ electron/s instead of $1.5 \cdot 10^{21}$ e/s) had no long-lived MH-OMs and the first ELM

often used to increase radial resolution on the pedestal measurements, and this could remove the resonant q from the flat-top of the pedestal. Further, the hybrid pulses have complicated plasma current waveforms, which again could displace the q resonance and terminate the mode. So far, only in the hot ion H-mode (when no radial drifts nor current ramps were applied) are there MH-OMs that last more than 100 ms: 13 of them. The average life-time of modes presented in Fig. 5 is 63 ms. The application of external error fields resulted in very brief MH-OMs, <20 ms when applied error field currents were > 1 kA (this is considered to be the minimum current required to observe effects on the plasma). Currents in the range 200-500 A show little statistical difference on MH-OM appearance when compared to zero current.

All the $n=1$ MH-OMs reported were seen in plasmas heated only by co-NBI, although they

occurred 1 s sooner, at 14.4 s. Note that the resistive current diffusion time for a 1 cm wide current ribbon at the pedestal top is of order 0.8 s (the ribbon is likely to be narrower, the resistive time faster). The long MH-OM shown in Fig. 1 lasts more than 1 s: a mechanism, yet unknown, is necessary for it to survive against resistive decay.

The power outflux to the outer divertor target was measured with a fast Infra-Red (IR) camera, viewing a narrow toroidal strip across the inner and outer target. During the long MH-OM of Fig. 1 the time averaged maximum heat flux varies from 25 MW/m^2 at mode onset, down to 17 MW/m^2 in its second half, to be compared with an ELMy-averaged maximum power outflux of 10 MW/m^2 in a later phase of the pulse. The ELMy average is calculated without compensating the strike point position shifts [8] that occur after and in between ELMs, so it is likely to be an under-estimate. For a different pulse the camera frame rate was especially set to $1/38 \mu\text{s}$ (26 kHz), with an integration time of $27 \mu\text{s}$, viewing only the outboard target (JET 77078, MH-OM from 14.28 to 14.355 s). In this case the fine structure of the power outflux footprint is revealed, as shown in Fig. 6. During the OM phase, periodic bursts of heat arrive away from the maximum deposition location, synchronised with magnetic blips. Both, overall transport across the pedestal and a time-localised (presumably toroidally localised) “hose-pipe” contribute to the increased outer target heat flux during the MH-OM, relative to the previous high confinement phase. The heat deposition observed could be consistent with the effect of a rotating current structure at the top of the pedestal: it could break toroidal symmetry and produce partial ergodisation of field lines further out in the pedestal gradient region, increasing overall particle and heat flux. Additionally, at a specific toroidal location in the gradient region (away from the current structure) a particular flux tube could escape through the broken separatrix (a homoclinic tangle, as described in [9]) and lead to the toroidally localised heat flux away from the main strike position shown in Fig. 6. But these considerations would be valid if the MH-OM had a tearing character. It is not clear if a kink-like instability (like the MH-OM) would also lead to the creation of a direct loss channel.

4. MHD models and relationship with other MHD modes

OMs have been identified as **external kinks** in Ref [3], driven by large current densities in the plasma gradient region. In that study the mode structure of the observed SXR fluctuations show a better match to the ideal $n=1$ external kink mode than to resistive modes. But the strong localization of the current feature at the source of the MH-OM (shown in Fig 3) is incompatible with the convective cell with a large poloidal extent mentioned in the article. Further, a preliminary analysis of ideal linear MHD shows that the plasma depicted in Fig. 1 is very stable to $n=1$ kinks, and we have identified experimentally that the mode is stably located at a rational surface at the pedestal flat-top, where the current density is likely to have a minimum (no bootstrap). Whether the nonlinear evolution of either tearing or kink modes might lead to a saturated mode comparable to the MH-OM is yet unknown.

From the experimental evidence described above we speculate that, given a low order rational at the pedestal top, either the high $T_{e,\text{ped}}$ (ideal MHD) and/or the high rotation shear present in the plasma before the mode onset lead to the circumstances necessary for localized current structure formation (closed MHD vortices), as implied in [10].

Comparison of pulses that have MH-OMs with matching pulses allows us to establish that ELM-free periods are prolonged by the presence of the MH-OM [11], which can survive

sawtooth crash events. On the other hand, MH-OMs can not survive ELMs. Further, ELMs that follow on a MH-OM are at least 30 % smaller, both in terms of the change in plasma diamagnetic energy and its impact on the position control system. When MH-OMs are present there is no evidence of **high n peeling-ballooning modes**, which are often seen to precede later ELMs in the same pulses. One of these high n modes with $n > 10$ is shown in red in Fig 1g, near $t = 15.5$ s, with mode frequency around 10 kHz.

Snakes are field-line aligned perturbations that have been observed in the core of tokamak plasmas, particularly near internal transport barriers, at $q=1$, $3/2$ or 2 . They have been modelled with localised current structures at the foot of an internal transport barrier [12], at minimum or maximum shear locations. A review by Wesson [6] already pointed out the intrinsic interest of such structures, which appear suddenly and can last more than expected by standard physics. The multi-harmonic OM could be said to be a “snake” at the top of the pedestal. Note that in both cases the mode appears where the pressure gradient is minimum or zero, leading to helicity conservation. Snakes can have either an excess or a defect of current relative to the background current distribution, and in all cases are reported to have a kink structure.

Palm-tree modes (PTM) are multi-harmonic ELM post-cursors [7]. They have been identified as “negative” co-rotating closed current filaments, produced by a plasma current defect. Analysis of SXR and ECE signals indicates a tearing character. The spectral characteristics of PTMs and MH-OMs are the same. In the presence of core MHD it is often not possible to ascertain the sign of the field blip, which would distinguish them. On the other hand, PTMs are known to appear in generally colder and denser plasmas than MH-OMs. It is speculated that a PTM reflects the loss of current from a particular flux tube due to the ELM. In that case one would expect to see palm-tree modes following the loss of an OM terminated by an ELM, but this has not been seen.

In our search for MH-OMs in the JET database we have encountered a number of long-lived PTMs. Usually the initial frequency of the fundamental is low, and soon rises to match the toroidal rotation frequency at the top of the pedestal, where it remains constant. Therefore, the PTM, like the MH-OM and the snake, is a field-aligned perturbation at a low order rational located at the pedestal flat-top, but always with a current deficit.

Dashboard modes are medium frequency multi-harmonic features propagating counter to the plasma rotation ($n < 0$) and located in the pedestal region [13,14]. They are not observed in conjunction with MH-OMs, but can coexist with PTMs. For instance, WBMs are shown in dark blue in Fig. 1g, in between brief interruptions of the MH-OM and after the 1st ELM.

5. Edge Harmonic Oscillation and the QH-mode

Long-lived OM in JET induce a plasma state very reminiscent of the Quiescent H-mode (QH-mode) [15,16], so named because it combines high confinement properties with the absence of ELMs. The MH-OM of JET may be related to the Edge Harmonic Oscillation (EHO) observed in QH-modes of DIII-D and AUG. Like the OM, the EHO produces a blip in the magnetic diagnostics and in the channels of the fluctuation diagnostics located in the pedestal gradient region, and replaces ELMs. So far there are no reports on the radial location of the current source that produces the EHO fluctuations, although it is argued that it must be located in the gradient region of the pedestal, where free energy is available to

drive the mode. This is not the case in our MH-OMs. In earlier reports the QH-mode was found to be associated with NBI counter-injection but more recent work [17] shows that it can now be obtained with either co or counter injection, as long as sufficient velocity shear is present.

The JET EHO, observed in counter NBI experiments and reported in [16] is quite different to the MH-OM described here. Reflectometry was used to identify it as an edge mode. However, in that case the dominant mode at 15 kHz is seen in ECE and SXR diagnostics as a core (1,1) mode which probably drives a small edge (3,1) perturbation detected by the reflectometer in the steep gradient region. Also, unlike the modes discussed here, it survives an ELM.

Conclusions

A field aligned co-current structure, co-rotating with the plasma and located at the top of the pedestal has been found to be the origin of the multi-harmonic Outer Mode. The MH-OM is only seen with sufficiently hot pedestal temperatures, which so far correspond to low or medium density at JET. All recent examples had co-injected NBI, although older experiments had already revealed counter-injected MH-OMs. The MH-OM, despite carrying very small current (~100-300 A) can have profound effects on the plasma pedestal, delaying or eliminating ELMs for considerable periods of time, and moderating the power outflux to the outer strike. It belongs to a family of modes found at regions of minimum pressure gradient.

Like the QH-mode, a quasi-steady H-mode as induced by the MH-OM in JET might be a potentially useful fusion operating regime, provided it can be controlled in a predictable manner, and it can exist at higher densities.

Acknowledgements:

We are grateful to Keith Burrell, Tim Hender, Tom Osborne, W. Suttrop, and D. Borba for useful discussions, and to Paul Carman for the 3D representation of a current ribbon.

This work was supported by EURATOM and carried out within the framework of the European Fusion Development Agreement, and under the contract of Association between EURATOM and the Laboratorio Nacional de Fusión, CIEMAT. The views and opinions expressed herein do not necessarily reflect those of the European Commission.

References

- [1] JET Team, presented by P.J. Lomas, *Plas. Phys. & Contr. Nucl. Fus. Res.* 1994 (Proc. 15th Int. Conf. Seville, 1994), Vol. 1, p. 211, IAEA, Vienna (1995).
- [2] Nave, M.F.F. et al., *Nucl. Fusion* 35 (1995) 409
- [3] Huysmans, G.T.A. et al., *Nucl. Fusion* 38 (1998) 179
- [4] Perez, C.P. et al., *Nucl. Fusion* 44 (2004) 609-623
- [5] Solano, E. R., et al., *Phys. Rev. Lett.* 104 (2010) 185003
- [6] Wesson, J.A., *Plasma Phys. Control. Fusion* 37 (1995) A337-346
- [7] Koslowski, H.R. et al; *Nucl. Fusion* 45 (2005) 201-208
- [8] Solano, E.R. et al., *Nucl. Fusion* 48 (2008) 065005
- [9] Evans, T.E. et al., *J. Phys.: Conf. Ser.* 7 (2005) 174

-
- [10] Petviashvili, V.I., Plasma Phys. Rep. 19 (1993) 256
 - [11] Nave, MFF. et al., Nucl. Fusion 39 (1999) 1567
 - [12] Alper, B. et al., 26th EPS Conf. on Contr. Fusion and Plasma Physics, Maastricht, 14 - 18 June 1999 ECA Vol.23J (1999) 173 - 176
 - [13] Smeulders P et al Plasma Phys. Control. Fusion 41 (1999) 1303
 - [14] Perez, C. P., et al., Plasma Phys. Control. Fusion 46 (2004) 61
 - [15] Burrell, K.H. et al., Phys. Plas., 12 (2005) 056121
 - [16] Suttrop, W. et al., Nucl. Fus. 45 (2005) 721
 - [17] Burrell, K.H. et al., Phys. Rev. Lett. 102 (2009) 155003